Protonation of the Cysteine Axial Ligand Investigated in His/Cys *c*-type Cytochrome by UV-Vis, Mid- and Far-IR Spectroscopy

Lidia Zuccarello[1,2,#], Catherine Berthomieu[1], Alain Boussac[3], Jean-Blaise Brubach[4], Irene Díaz-Moreno[5], Antonio J. Díaz Quintana[5], Rainer Hienerwadel[2*]*

[1] CEA, CNRS, Aix Marseille Univ., BIAM, Interactions Protéine Métal UMR 7265, 13108 Saint Paul-Lez-Durance, France

[2] Aix Marseille Univ., CEA, CNRS, BIAM, Luminy Genetics and Biophysic of Plants, UMR 7265, 13288 Marseille Cedex, France

[3] I2BC, UMR CNRS 9198, CEA Saclay, 91191 Gif-sur -Yvette, France.

[4] Synchrotron SOLEIL, AILES Beamline, L'Orme des Merisier, Saint-Aubin, BP 48, F-91192 Gif-sur-Yvette Cedex, France

[5] Instituto de Investigaciones Químicas (IIQ), Centro de Investigaciones Científicas Isla de la Cartuja (cicCartuja), Universidad de Sevilla – Consejo Superior de Investigaciones Científicas (CSIC), Avda. Américo Vespucio 49, Sevilla 41092, Spain

[#]Current address: Instituto de Tecnologia Quimica e Biologica (ITQB), Universidade Nova de Lisboa, Av. da Republica (EAN), 2780-157 Oeiras, Portugal.

Corresponding Authors: * Catherine Berthomieu: catherine.berthomieu@cea.fr. * Rainer Hienerwadel: rainer.hienerwadel@univ-amu.fr.

His/Cys coordination was recently found in several *c*-type cytochromes, which could act as sensors, in electron transport or in regulation. Towards better understanding Cys function and reactivity in these cytochromes, we compare cytochrome c6 (c6wt) from the cyanobacterium *Nostoc* PCC 7120 with its Met58Cys mutant. We probe the axial ligands and heme properties by combining visible and Mid to Far FTIR difference spectroscopies. Cys58 determines the strong negative redox potential and pH dependence of M58C (E_{mM58C} = -375 mV, *versus* E_mc6wt = +339 mV). Mid-IR (notably *Cys ν(SH), His ν(C_5N_1), heme δ(CmH)*) and Far-IR (*ν(Fe(II)-His), ν(His-Fe(III)-Cys)*) markers of the heme and ligands show that Cys58 remains a strong thiolate ligand of reduced Met58Cys at alkaline pH, while it is protonated at pH 7.5, stabilized by a strong hydrogen bonding interaction, and weakly interacts with Fe(II). These data provide a benchmark for further analysis of *c*-type cytochromes with natural His/Cys coordination.

TOC GRAPHICS

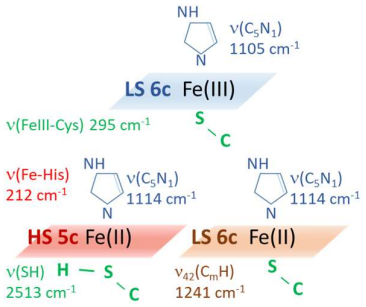

KEYWORDS : Cysteine protonation, Mid- and Far- infrared, c-type Cyt, His/Cys coordination

Cysteine coordination as an axial metal ligand plays an essential role in the reactivity of many oxidoreductases, such as superoxide reductases, Ni-superoxide dismutase, or heme-containing monooxygenases. The Cys-Metal bond strength and the protonation state of coordinated Cys - at times - are critical for the catalytic function of these enzymes [1-4] .

Recently, a growing number of natural *c*-type cytochromes (Cyt) with histidine/cysteine axial coordination have been discovered [5-12], including two Cyt with a Per-Arnt-Sim (PAS) molecular sensor domain, Tll0287 from *T. elongatus* and the transcriptional regulator RcoM [10,13-15], which indicates a role of these Cyt in signalling. His/Cys axial coordination is rare in Cyt, the sixth axial iron ligand being most commonly a methionine or a histidine, and less frequently a tyrosine. Besides modulating the heme midpoint potential, redox- or substrate- induced changes in the protonation state of the sixth Cys axial ligand could be eventually critical for the function of these proteins. Further, Cys are prone to post-translational modifications such as nitrosylation or persulfidation, raising the question of the reactivity of Cys ligands for some cytochromes, particularly those involved in sulfur metabolisms [6,8,16].

Scant data are available regarding the His/Cys axial coordination in *c*-type Cyt and the thiol versus thiolate Cys coordination, besides some reports on semisynthetic cytochrome *c* (cyt*c*) or cyt*c* site-directed mutants [17,18]. EPR and UV-Vis spectroscopy are good probes of Cys coordination in oxidized Cyt. In contrast, reduced His/Cys Cyt are EPR silent and their UV-Vis spectra ambiguous. Data on thiolate-bound, six-coordinated (6c) Fe(II) hemes were only evidenced upon the addition of exogenous sulphur-containing ligands to hemoproteins [4,19]. It was recently proposed a possible coordination of a reduced heme by a thiol ligand [4]. However, the UV-Vis spectral features hardly allow to distinguish Fe(II) coordination by a protonated Cys thiol from coordination by other neutral ligands.

In this context, our work aims at pinpointing physicochemical properties of His/Cys axial coordination in c-type Cyt, by combining UV-Vis spectroscopy and Mid- and Far-IR FTIR difference spectroscopy coupled to electrochemistry. With infrared spectroscopy, we directly probe Cys

protonation by following the Cys ν(SH) IR mode [20], the heme iron coordination using previously identified IR markers of the iron spin state [21-23], and the histidine ligand [22,24-26]. We also identify new Far-IR markers of the His/Cys coordination. We have pursued a comparative study between cytochrome *c*6 (c6wt) of the cyanobacterium Nostoc PCC7120 having His18/Met58 coordination and its His18/Cys58 site-directed mutant (M58C). This system is particularly interesting since three-dimensional structures showed the absence of significant structural changes of the rest of the protein upon the Met58Cys mutation (c6wt, structure PDB: 4GYD and M58C, structure PDB: 4H0J, Scheme 1 [27]). Studies at neutral and alkaline pH allowed to probe Cys(SH) versus Cys(S^-) coordination of the ferrous heme and to obtain spectroscopic markers of these forms, which are relevant to His/Cys *c*-type Cyt properties and function.

SCHEME 1: A) Structure of c6wt (4GYD), B) Structure of M58C (4H0J) [27].

The N(His18)-Fe distances are 2.05 Å in c6wt and 2.15 Å in M58C; the Fe-S(Met58) is 2.28 Å in c6wt and the Fe-S(Cys58) is 3.28 Å in M58C.

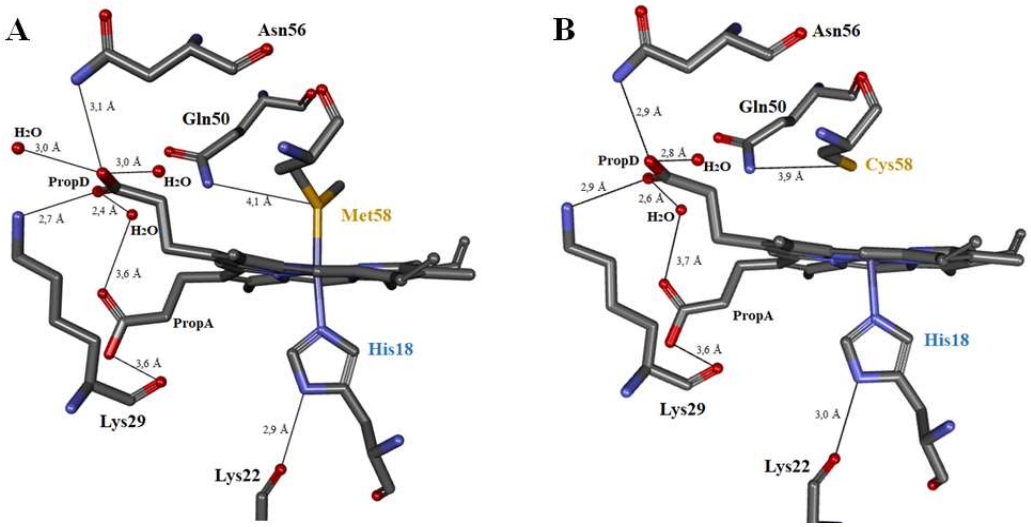

UV-Vis spectroscopy:

The Soret band of the M58C in its oxidized state ($M58C_{OX}$) exhibits a characteristic and specific red shift when compared to that of $c6wt_{OX}$ (+8 nm from 410 nm to 418 nm at pH 7.5, Figure 1 and Table 1). This red shift has been previously described for oxidized cyt*c* variants with His/Cys coordination [17,18]. Shifts of the Q bands are also evident, as well as two CysS-Fe(III) charge transfer bands at ≈ 655 nm and ≈ 745 nm (Figure 1A, inserts) in M58C, characteristic of thiolate- coordinated Fe(III) hemes [17,18,28,29] [1]. Reduction of c6wt is accompanied by a 6-nm red shift and hyperchromic effect of the Soret band, as expected for Cyt with His/Met coordination. In contrast, the Soret band peaks at almost the same wavelength for $M58C_{OX}$ and $M58C_{RED}$, and there is a minimum increase in the Soret band intensity for $M58C_{RED}$ (Figure 1A). This UV-Vis spectrum does not give clear information on the axial Cys coordination to $M58C_{RED}$.

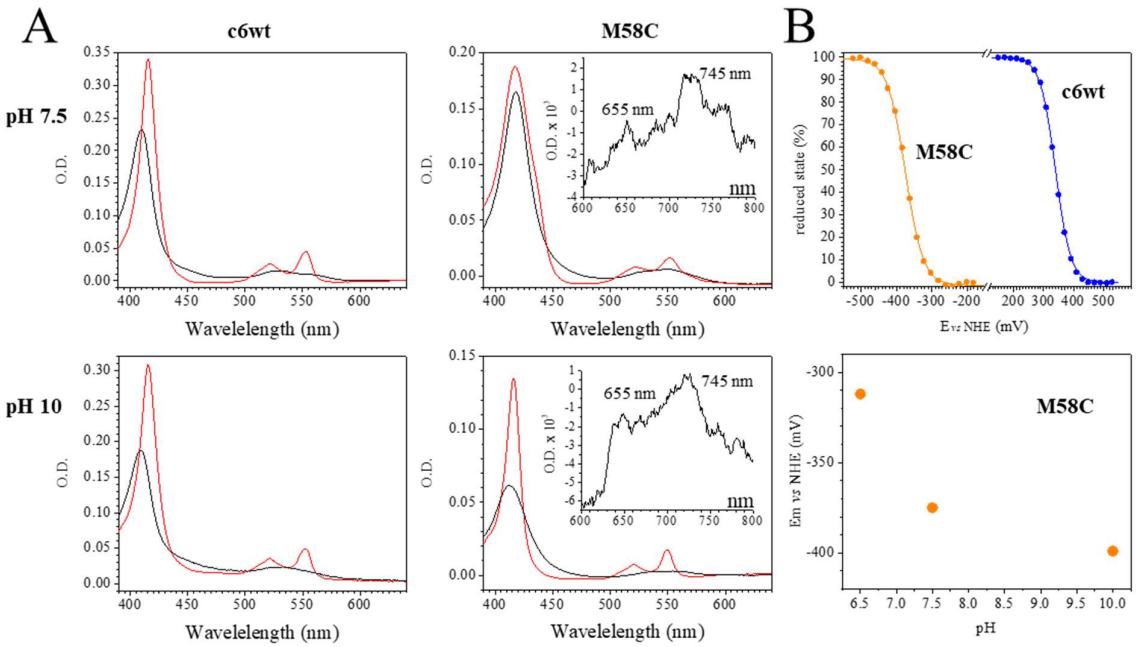

FIGURE 1: A) UV-visible absorption spectra of c6wt (left) and M58C (right) in the reduced (red) and oxidized (black) states at pH 7.5 (top) and at pH 10 (bottom). The spectra were recorded in the FTIR electrochemical cell, *i.e.* under conditions in which the concentration and thickness of the

[1] These bands of very small amplitudes were revealed in the oxidized – *minus* – reduced spectrum obtained by spectro-electrochemistry, as detailed in Sup. Mat.

samples are difficult to be precisely adjusted. This is why the absorption intensity slightly differs in the samples. B - top) Redox titration performed by spectro-electrochemistry in the UV-Vis range with c6wt (blue points) and M58C (orange points) at pH 7.5. The proportions of the reduced state estimated has been estimated from the amplitudes of the Soret bands and Q bands. They were fitted with a Nernst equation (continuous lines) with n fixed to 1. B-bottom) pH dependence of M58C midpoint potential.

By changing the pH, no significant spectral modifications are observed for oxidized or reduced c6wt (Figure 1). The spectral properties of $M58C_{OX}$ are also only slightly affected by pH and the two CysS-Fe(III) charge transfer bands at 655 and 745 nm clearly show that $M58C_{OX}$ maintains a thiolate coordination between pH 7.5 and 10. The main change concerns $M58C_{RED}$, with a larger amplitude and smaller bandwidth of the Soret band at pH 10 as compared to pH 7.5. These data point to a pH-sensitive axial coordination of $M58C_{RED}$.

The effect of pH on the heme coordination in M58C was further analysed using spectro-electrochemical titrations in the UV-Vis range. The midpoint potentials of c6wt and M58C were determined at +339 and -374 mV *vs* NHE, respectively, at pH 7.5 (Figure 1B, upper panel, data are summarized in Table S1). Mutation of the 6th axial iron ligand from Met to Cys causes a decrease by *circa* 700 mV of the midpoint potential of the heme iron. This is in line with the result obtained on semisynthetic cyt *c* with His/Cys coordination [17]. Interestingly, the midpoint potential of M58C depends on pH with a *circa* -60 mV/pH unit between pH 6.5 and 7.5 (Figure 1B, lower panel), indicating the deprotonation of a residue upon M58C oxidation in this pH range. The effect of pH on the midpoint potential is smaller above pH 7.5, with Em calculated at -399 mV at pH 10[2]. These data indicate a pK_{RED} value comprised between 8 and 9 for the protonatable group, indicating that it is deprotonated both in the oxidized and reduced forms at alkaline pH values.

[2] The data at pH 10 could not be fitted by a Nernst curve with n=1. This likely originates from an electrostatic interaction between hemes of different cytochromes. The Em has been calculated taking into account a fraction of M58C associated in dimers, as detailed in Figure S1.

Mid- and Far-IR FTIR difference spectroscopy:

To identify this group and dig into the coordination properties and structural changes associated to the redox activity of c6wt and M58C, we performed electrochemically-induced FTIR difference spectroscopy. This spectroscopy directly probes the properties of amino acid side-chains and polypeptide backbone. Actually, for *b*-type or *c*-type Cyt with His/His or His/Met coordination, thorough investigation of model compounds evidenced typical redox- and spin state- sensitive IR features of the heme and signatures of the 5th histidine ligand [21-23,30-33].

Besides difference bands associated to the polypeptide backbone and amino acid side chains in the 1700-1600 cm^{-1} region (detailed in Supp. Figure S2), contributions from the heme and axial ligands are clearly detected in the reduced – *minus* – oxidized FTIR difference spectra recorded with c6wt and M58C (Figure 2).[3] For example, bands at 1534 cm^{-1} and 1239 cm^{-1} in the spectrum recorded with c6wt at pH 7.5 are assigned to the heme modes $\nu_{38}(C_bC_b)$ and $\nu_{42}(C_mH)$ of $c6wt_{RED}$. The complete band assignments are summarized in Supp. Table S2 [21,22]. A number of resonance Raman (RR) markers of *c*-type heme coordination and spin states have been reported [34,35]. However, they are either not IR active or not redox sensitive, and thus not observable in the redox-induced FTIR difference spectra. Nevertheless, we previously showed that the $\nu_{42}(\delta C_mH)$ heme mode is a typical detectable marker for a six-coordinated low spin (6c LS) Fe(II) heme using FTIR difference spectroscopy [22]. The IR signature of the 5th His ligand is observed with the $\nu(C_5N_1)$ mode at 1118 cm^{-1} for $c6wt_{RED}$ and at 1103 cm^{-1} for $c6wt_{OX}$ [21,22,25,26]. The frequency of this mode is sensitive to the protonation-state of the His ligand and indicates here that the histidine ligand is neutral for both redox states [21,25,26]. The difference band at 1748 ($c6wt_{OX}$) / 1733 ($c6wt_{RED}$) cm^{-1} corresponds to the redox sensitive band shift of a protonated carboxylic group. It could be due to a protonated heme propionate [36], or alternatively, to a protonated Asp or Glu residue.

[3] The assignment of infrared bands have been made by comparison with literature data as well as with previous data obtained on model compounds. It also resides on the typical band frequency shifts observed in spectra recorded with samples in ^2H_2O (Figure S1). Details on the assignment are given in Supplemental Material.

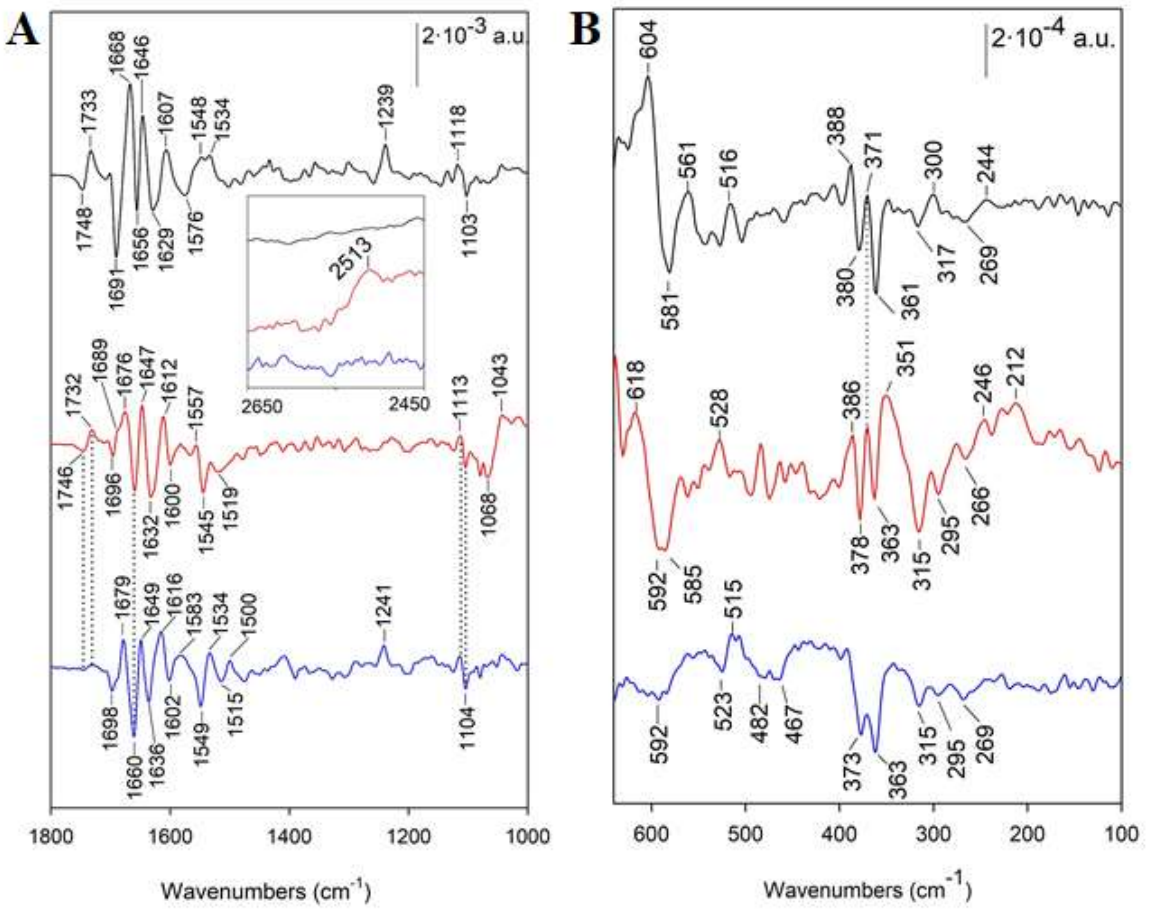

FIGURE 2: Reduced – *minus* – oxidized FTIR difference spectra between 1800 and 1000 cm^{-1} (A), 2700 and 2450 cm^{-1} (insert in panel A) and between 650-100 cm^{-1} (B). Spectra were recorded with c6wt at pH 7.5 in A and pH 5.5 in B (black lines), with M58C at pH 7.5 in A and pH 5.5 in B (red lines) and M58C at pH 10 in A and pH 11 in B (blue lines).

The spectrum recorded with M58C at pH 7.5 exhibits overall similarity with that of c6wt in the 1700-1600 cm^{-1} range indicating similar redox-induced structural changes of the protein. The difference band assigned to a protonated carboxylic group is also present, at 1746/1732 cm^{-1}, in M58C. Changes in protonation of propionate groups have been previously associated to the pH dependence of cytochrome's midpoint potentials [37]. The difference band observed here, and the clear band downshift observed in ^2H_2O (Figure S2) show that the carboxylic group is protonated both for $M58C_{RED}$ and $M58C_{OX}$ and is not responsible for the pH dependence of M58C midpoint potential.

There are three particular spectral differences in the spectrum recorded with M58C. Firstly, there is no equivalent of the $\nu_{42}(\delta C_mH)$ mode at ≈ 1239 cm^{-1} for $M58C_{RED}$ at pH 7.5, which indicates that the Fe(II) heme is not 6c LS. Secondly, the $\nu(C_5N_1)$ mode of the 5th histidine ligand His18 is observed at 1113 cm^{-1} for $M58C_{RED}$, i.e. downshifted by 4 cm^{-1} when compared to $c6wt_{RED}$. The frequency of the $\nu(C_5N_1)$ mode still indicates that the His ligand is neutral in $M58C_{RED}$. The lower frequency of this mode indicates a stronger Fe^{2+}–N_1 interaction. This may be due to the differences in coordination properties of the heme iron, as well as to different properties of the hydrogen bonding interactions described between His18 side-chain and the peptide carbonyl of Lys21 in the structures of both M58C and c6wt (Scheme 1) [27]. Thirdly, a positive band is observed at 2513 cm^{-1} for $M58C_{RED}$ only (Figure 2 insert). This band, downshifted to 1833 cm^{-1} in ^2H_2O, is assigned to the ν(SH) mode of a Cys side-chain (Supp. Figure S2 [38,39]).

We thus conclude that the Cys axial ligand of M58C becomes protonated upon heme reduction, since Cys58 is the only Cys residue of the protein not involved in covalent linkage of the heme. The Cys58 ν(SH) mode frequency is at the lower limit of those reported in the literature for thiols involved as donors in very strong hydrogen bonds [40-43]. Since the structural data on M58C (Scheme 1) evidence an interaction between Cys58 and Gln50, we propose that the protonated Cys58 interacts with the carbonyl group of Gln50 in $M58C_{RED}$. Note that, although in Scheme 1, the Gln50 amine group points towards the Cys thiol, the other conformer with the carbonyl group pointing towards the SH could also be fitted in the electron density (not shown). The unusually low frequency of the Cys ν(SH) mode further indicates that an electrostatic interaction persists between the Cys sulphur and the reduced heme iron. The absence of the IR $\nu_{42}(\delta C_mH)$ marker of the 6c LS ferrous heme indicates that no alternative protein ligand replaces Cys58 and that CysSH forms only a weak interaction with the heme. In addition, bands at 1068/1043 cm^{-1}, assigned to the Tris buffer (Supp. Figure S4), indicate a proton transfer from the buffer to M58C upon M58C reduction. This proton uptake may correspond to the protonation of the 6th axial ligand Cys58 upon M58C reduction and explain the pH dependence of the M58C midpoint potential.

Identical FTIR data have been obtained with M58C at pH 5.5 to 7.5 (Figure S3), while at pH 10, the positive ν(SH) band, seen at 2519-2513 cm^{-1} at lower pH values, is absent and the $\nu_{42}(\delta C_mH)$ heme mode is observed at 1241 cm^{-1} (Figure 2A). This shows that the Cys58 remains a strong deprotonated ligand of a 6c LS Fe(II)-iron in $M58C_{RED}$ at alkaline pH. The IR signature of the 5th His ligand (1113 cm^{-1} for $M58C_{RED}$ and 1104 cm^{-1} for $M58C_{OX}$) remains the same at low and at alkaline pH, indicating the same properties of interaction with the heme.

We further probed the spectral signatures of the His/Met and His/Cys coordination in the Far-IR range (650 and 100 cm^{-1}, Figure 2B). In this spectral region, heme skeletal modes are expected to contribute, as well as modes involving interactions of the heme iron with the axial ligands. Bands assignments for the Far-IR FTIR difference spectra recorded for the first time with *c*-type Cyt with His/Cys axial coordination are summarized in Table 2 (data analysis is detailed in Supp. Data S3).

In the IR spectra of metalloporphyrins, in-plane (ip) Fe-Npyrrole stretching and out-of-plane (oop) pyrrole tilting/folding modes ν8 and ν50 give rise to intense bands in the 420-350 cm^{-1} region ([23,32,33,44-48] and references therein). These bands are identified at 388 and 371 cm^{-1} for the reduced forms and at 380-373 and 363-361 cm^{-1} for the oxidized forms of c6wt and M58C, respectively (Figure 2B). These modes are likely coupled with Fe-axial ligands vibrations [23]. However, the band frequencies are only slightly affected by the change of His/Met to His/Cys coordination at pH 7.5. At alkaline pH, the band at 371 cm^{-1} is absent in $M58C_{RED}$ and the band at 378 cm^{-1} is downshifted by 5 cm^{-1} in $M58C_{OX}$. Bands at 317 and 269 cm^{-1} for $c6wt_{OX}$ are observed at almost the same frequency for $M58C_{OX}$ at neutral and alkaline pH. Since these bands were also detected for cyt *c*, they are tentatively assigned to heme modes, by comparison with resonance Raman data [49].

A main difference between spectra recorded with c6wt and M58C in the Far-IR region consists in an additional band at 295 cm^{-1} in $M58C_{OX}$ (Figure 2B red and blue lines). Since a Fe-S stretching mode involving the axial Cys ligand was reported by resonance Raman at 312 cm^{-1} for the His/Cys 6c LS Fe(III) *b*-type heme of cystathionine β-synthase using ^{34}S-labeling [50], we confidently assign

the new negative band at 295 cm^{-1} for $M58C_{OX}$ to a ν_{as}(HisFe(III)Cys) mode, marker of His-Fe(III)-Cys coordination. As for resonance Raman, no equivalent mode is detected for the reduced heme [50].

Another specificity of the spectrum recorded with M58C in the Far-IR region consists in bands at 351 cm^{-1} and 220-212 cm^{-1} for $M58C_{RED}$ at low pH (Figure 2B red line), which are absent in the spectrum recorded at alkaline pH (Figure 2B blue line). Resonance Raman literature data assigned unambiguously a band at 222-218 cm^{-1} to the ν(Fe(II)-His) mode of the 5c- Fe(II) heme in myoglobin and haemoglobin [51-53]. Given the results obtained in the Mid-IR, we assign the band at 220-212 cm^{-1} in Figure 2B to the ν(Fe(II)-His) IR mode of the 5c Fe(II)-heme in $M58C_{RED}$. Cys protonation in this 5c Fe(II) M58C is expected to alter the heme conformation, and the coupling of ip (in plane) and oop (out of plane) heme modes with modes involving the Fe-axial ligand. Actually, an oop pyrrole tilting mode at 243 cm^{-1} was enhanced specifically in the 5c- Fe(II) heme of myoglobin, pointing a specific structure of the heme-His geometry in this protein [53]. This suggests that the band at 246 cm^{-1} for $M58C_{RED}$ is an oop pyrrole heme mode, enhanced upon 5c- Fe(II) coordination. The band at 351 cm^{-1} also could result from changes in the heme properties. However, we cannot exclude a contribution of the Cys thiol at this frequency since a band at 346-364 cm^{-1} was assigned to a S–H oop bending mode of L-cysteine [54]. The disappearance of the positive bands at 351 and 212 cm^{-1} in the FTIR difference spectrum recorded with M58C at pH 11 is explained by the different coordination, with cysteinate remaining as a strong 6th ligand of $M58C_{RED}$.

At pH 7.5, strong difference bands are observed at 604/581 cm^{-1} for c6wt (Figure 2B black line) and at 618/592 cm^{-1} for M58C (Figure 2B red line). These bands are absent at alkaline pH (Figure 2B blue line). They are tentatively assigned to the δCOO_{sciss} mode of a protonated carboxylic group by comparison with literature data [55,56], and because the disappearance of these bands at alkaline pH is in line with that of the Mid-IR bands characteristic of the protonated carboxylic group at 1746/1732 cm^{-1} (Figure 2A, blue line).

The structures of c6wt and M58C (Scheme 1 [27]) show very similar environments for the 5th histidine ligands, which form a hydrogen-bond interaction with a Lysine side-chain, and for the

propionate groups, involved in similar hydrogen bonding networks. Met58 substitution by Cys thus induces modest structural changes in the heme environment. Interestingly, the Fe-S(Cys) distance in the X-ray structure of the M58C mutant is rather long (3.28 Å). This suggests that reduction of the heme occurred in the X-ray beam, so that the structure of M58C is that of a 5c- Fe(II) heme with Cys58 protonated, as revealed by FTIR spectroscopy. This structure recorded at cryogenic temperature probably does not exactly correspond to that of $M58C_{RED}$ at room temperature. However, it supports a model in which a hydrogen bonding interaction between Cys58 and Gln50 side-chains could stabilize the protonated CysSH above the heme iron, preventing the coordination of another residue. Interestingly, redox sensitive IR bands identified upon M58C reduction at 1688 cm^{-1} are assigned to a Gln side-chain, as detailed in Figure S2, and could correspond to a change in Gln50-Cys58 interaction, following Cys58 protonation.

In conclusion, few examples of cytochromes with His/Cys axial coordination exist and spectroscopic investigations are needed to identify their coordination properties, and the reactivity of the Cys ligand. Comparing the redox sensitive UV-Vis and IR properties of c6wt and its M58C mutant, we directly probed the axial ligands, obtained spectroscopic markers of Cys protonation and associated heme-iron coordination properties, which will be useful to study *c*-type Cyt with His/Cys coordination. Direct detection of the mid-IR Cys ν(SH) mode demonstrated the redox-sensitive change in the Cys ligand protonation. Concomitant with Cys58 protonation, the loss of an IR marker of 6c LS Fe(II) heme upon M58C reduction, and the identification of a new ν(FeII-His) mode in the Far-IR, indicated the formation of a 5c- Fe(II) heme [52,53]. The crystallographic structure obtained for M58C further indicated that 5c- $M58C_{RED}$ is stabilized by a strong interaction between the Cys58S-H and a neighbouring Gln. We propose that such a structural configuration may be critical to prevent ligand switching and hence to enable reactivity of the Cys axial ligand in cytochromes with natural

His/Cys coordination and/or the accessibility of Fe(II) to exogenous ligands, in relation with a Cyt signalling function.

The new Mid- and Far-IR markers of His/Cys^- *versus* His/CysH coordination identified in M58C, and more generally the combined use of UV-Vis and Mid/Far - FTIR difference spectroscopy are very promising to investigate the structural properties of *c*-type Cyt with natural His/Cys coordination, and to infer their specific role as electron transfer or sensors *in vivo.*

Experimental Section

C6wt and M58C were purified as previously described [27]. Spectro-electrochemistry was performed using a vacuum-tight three-electrode thin path-length cell [57] equipped with CaF_2 or chemical vapor deposition (CVD) diamond windows and externally triggered by a potentiostat EG&G 262 or by a Tacussel potentiostat Type PRGE. Mid-IR data were recorded using Bruker Tensor 27, or IFS66s spectrophotometers equipped with KBr beam splitters, MCT or DTGS detectors. Far-IR FTIR data were recorded on a Bruker Vertex 70v equipped with Si beam splitters and 4.2 K Si-Bolometer. Experimental details on sample preparation, redox mediators, and spectral acquisition are given in supporting information.

Acknowledgements

AB, CB, JBB, LZ, and RH acknowledge support by the French Agence Nationale de la Recherche (ANR) under grant PSIIFIR ANR-15-CE05-0016. AB was supported in part by the French Infrastructure for Integrated Structural Biology (FRISBI) ANR-10-INBS-05. IDM and ADQ were funded by the Spanish Ministry of Science and Innovation / FEDER−National Research Agency (PGC2018-096049-B-I00), European Social Fund, Andalusian Government (BIO-198, US-1257019 and US-1254317).

Supplementary information.

Experimental Section

Supplementary Figure S1 Titration curves for A) c6wt and B) M58C at pH 6.5 (black) and pH 10 (red).

Supplementary Figure S2: Effect of $H_2O/^2H_2O$ exchange at pH 7.5 on the reduced – *minus* – oxidized FTIR difference spectra

Supplementary Figure S3: Effect of pH on the reduced – *minus* – oxidized difference spectra recorded with M58C in the 1800-1000 cm^{-1} range.

Supplementary Figure S4: Effect of M58C reduction on Tris buffer

Supplementary Table S1: Midpoint potentials of c6wt and M58C. Potentials are expressed in mV *versus* NHE

Supplementary Table S2: Proposed assignments of M58C bands in the Mid-IR difference spectra; shifts in ^2H_2O are given under brackets.

Supplementary data S3: Detailed assignment of the redox-sensitive Far-IR modes of c6wt and M58C.

Tables

Table 1: Maxima of the Soret and Q bands of c6wt and M58C at pH 7.5 and pH 10. Wavelengths are expressed in nm.

	pH 7.5			pH 10		
	Soret band	Q bands	CT bands	Soret band	Q bands	CT bands
$c6wt_{OX}$	410	~ 529		409	~ 531	
$M58C_{OX}$	418	~ 549	~ 655, ~ 745	416	~ 554	~ 655, ~ 745
$c6wt_{RED}$	416	522 / 553		415	522 / 552	
$M58C_{RED}$	417	523 / 551		416	520 / 549	

Table 2: Redox-sensitive Far-IR modes of c6wt and M58C and proposed assignments. The data are expressed in wavenumbers (cm^{-1}).

C6wt pH 5.5		M58C pH 5.5		M58C pH 11		Proposed assignments
Ox	Red	Ox	Red	Ox	Red	
581	604	593	618	-	-	δ(OCO) of COOH (Asp/Glu or Propionic acid)
380	388	378	386	373	386	ν_8(Fe-$N_{4\text{-}Pyr}$)
361	371	363	371	363	-	ν_{50}(Fe-$N_{4\text{-}Pyr}$)
	-		351		-	δ(SH) or ν(Fe-N_{pyr})
317	300	315		315		$\gamma 7(C_\alpha C_m) + \nu_{51}(\delta C\beta C1)_{as}$
-		295		295		ν(His-Fe(III)-Cys)
269	244	266	246	269	-	$\nu_{52}(\delta C_\beta C_1)_s$
			220-212		-	ν(FeII-His)

References

(1) Mathe, C.; Weill, C. O.; Mattioli, T. A.; Berthomieu, C.; Houee-Levin, C.; Tremey, E.; Niviere, V. Assessing the Role of the Active-Site Cysteine Ligand in the Superoxide Reductase from *Desulfoarculus baarsii*. *J. Biol. Chem.* **2007**, *282*, 22207-22216. DOI: 10.1074/jbc.M700279200

(2) Szilagyi, R. K.; Bryngelson, P. A.; Maroney, M. J.; Hedman, B.; Hodgson, K. O.; Solomon, E. I. S. K-edge X-Ray Absorption Spectroscopic Investigation of the Ni-Containing Superoxide Dismutase Active Site: New Structural Insight into the Mechanism. *J. Am. Chem. Soc.* **2004**, *126*, 3018-3019. DOI: 10.1021/ja039106v

(3) Dunford, A. J.; McLean, K. J.; Sabri, M.; Seward, H. E.; Heyes, D. J.; Scrutton, N. S.; Munro, A. W. Rapid P450 Heme Iron Reduction by Laser Photoexcitation of *Mycobacterium tuberculosis* CYP121 and CYP51B1 - Analysis of CO Complexation Reactions and Reversibility of the P450/P420 Equilibrium. *J. Biol. Chem.* **2007**, *282*, 24816-24824. DOI: 10.1074/jbc.M702958200

(4) Sono, M.; Sun, S. F.; Modi, A.; Hargrove, M. S.; Molitor, B.; Frankenberg-Dinkel, N.; Dawson, J. H. Spectroscopic Evidence Supporting Neutral Thiol Ligation to Ferrous Heme Iron. *J. Biol. Inorg. Chem.* **2018**, *23*, 1085-1092. DOI: 10.1007/s00775-018-1611-3

(5) Alric, J.; Tsukatani, Y.; Yoshida, M.; Matsuura, K.; Shimada, K.; Hienerwadel, R.; Schoepp-Cothenet, B.; Nitschke, W.; Nagashima, K. V. P.; Vermeglio, A. Structural and Functional Characterization of the Unusual Triheme Cytochrome Bound to the Reaction Center of *Rhodovulum sulfidophilum*. *J. Biol. Chem.* **2004**, *279*, 26090-26097. DOI: 10.1074/jbc.M400361200

(6) Brito, J. A.; Denkmann, K.; Pereira, I. A. C.; Archer, M.; Dahl, C. Thiosulfate Dehydrogenase (TsdA) from *Allochromatium vinosum*: Structural and Functional Insights into Thiosulfate Oxidation. *J. Biol. Chem.* **2015**, *290*, 9222-9238. DOI: 10.1074/jbc.M114.623397

(7) Grein, F.; Venceslau, S. S.; Schneider, L.; Hildebrandt, P.; Todorovic, S.; Pereira, I. A. C.; Dahl, C. DsrJ, an Essential Part of the DsrMKJOP Transmembrane Complex in the

Purple Sulfur Bacterium *Allochromatium vinosum*, Is an Unusual Triheme Cytochrome c. *Biochemistry* **2010**, *49*, 8290-8299. DOI: 10.1021/bi1007673

(8) Kappler, U.; Maher, M. J. The Bacterial SoxAX Cytochromes. *Cell. Mol. Life Sci.* **2013**, *70*, 977-992. DOI: 10.1007/s00018-012-1098-y

(9) Kerfeld, C. A.; Sawaya, M. R.; Bottin, H.; Tran, K. T.; Sugiura, M.; Cascio, D.; Desbois, A.; Yeates, T. O.; Kirilovsky, D.; Boussac, A. Structural and EPR Characterization of the Soluble Form of Cytochrome c-550 and of the psbV2 Gene Product from the Cyanobacterium *Thermosynechococcus elongatus*. *Plant Cell. Physiol*. **2003**, *44*, 697-706. DOI: 10.1093/pcp/pcg084

(10) Smith, A. T.; Marvin, K. A.; Freeman, K. M.; Kerby, R. L.; Roberts, G. P.; Burstyn, J. N. Identification of Cys(94) as the Distal Ligand to the Fe(III) Heme in the Transcriptional Regulator RcoM-2 from *Burkholderia xenovorans*. *J. Biol. Inorg. Chem.* **2012**, *17*, 1071-1082. DOI: 10.1007/s00775-012-0920-1

(11) Suga, M.; Lai, T. L.; Sugiura, M.; Shen, J. R.; Boussac, A. Crystal Structure at 1.5 Angstrom Resolution of the PsbV2 Cytochrome from the Cyanobacterium *Thermosynechococcus elongatus*. *FEBS Lett.* **2013**, *587*, 3267-3272. DOI: 10.1016/j.febslet.2013.08.023

(12) Ukita, S.; Fujii, T.; Hira, D.; Nishiyama, T.; Kawase, T.; Migita, C. T.; Furukawa, K. A Heterodimeric Cytochrome c Complex with a Very Low Redox Potential from an Anaerobic Ammonium-Oxidizing Enrichment Culture. *FEMS Microbiol. Lett.* **2010**, *313*, 61-67. DOI: 10.1111/j.1574-6968.2010.02122.x

(13) Boussac, A.; Koyama, K.; Sugiura, M. The Tll0287 Protein is a Hemoprotein Associated with the PsbA2-Photosystem II Complex in *Thermosynechococcus elongatus*. *Biochim. Biophys. Acta* **2013**, *1827*, 1174-1182. DOI: 10.1016/j.bbabio.2013.06.002

(14) Marvin, K. A.; Kerby, R. L.; Youn, H.; Roberts, G. P.; Burstyn, J. N. The Transcription Regulator RcoM-2 from *Burkholderia xenovorans* is a Cysteine-Ligated Hemoprotein that Undergoes a Redox-Mediated Ligand Switch. *Biochemistry* **2008**, *47*, 9016-9028. DOI: 10.1021/bi800486x

(15) Motomura, T.; Suga, M.; Hienerwadel, R.; Nakagawa, A.; Lai, T. L.; Nitschke, W.; Kuma, T.; Sugiura, M.; Boussac, A.; Shen, J. R. Crystal Structure and Redox Properties of a

Novel Cyanobacterial Heme Protein with a His/Cys Heme Axial Ligation and a Per-Arnt-Sim (PAS)-Like Domain. *J. Biol. Chem.* **2017**, *292*, 9599-9612. DOI: 10.1074/jbc.M116.746263

(16) Reijerse, E. J.; Sommerhalter, M.; Hellwig, P.; Quentmeier, A.; Rother, D.; Laurich, C.; Bothe, E.; Lubitz, W.; Friedrich, C. G. The Unusal Redox Centers of SoxXA, a Novel C-type Heme-Enzyme Essential for Chemotrophic Sulfur-Oxidation of *Paracoccus pantotrophus*. *Biochemistry* **2007**, *46*, 7804-7810. DOI: 10.1021/bi7003526

(17) Raphael, A. L.; Gray, H. B. Semisynthesis of Axial-Ligand (Position-80) Mutants of Cytochrome-C. *J. Am. Chem. Soc.* **1991**, *113*, 1038-1040. DOI: 10.1021/ja00003a045

(18) Zhong, F. F.; Lisi, G. P.; Collins, D. P.; Dawson, J. H.; Pletneva, E. V. Redox-Dependent Stability, Protonation, and Reactivity of Cysteine-Bound Heme Proteins. *Proc. Natl Acad Sci. USA* **2014**, *111*, 306-315. DOI: 10.1073/pnas.1317173111

(19) Perera, R.; Sono, M.; Sigman, J. A.; Pfister, T. D.; Lu, Y.; Dawson, J. H. Neutral Thiol as a Proximal Ligand to Ferrous Heme Iron: Implications for Heme Proteins that Lose Cysteine Thiolate Ligation on Reduction. *Proc. Natl. Acad. Sci. USA* **2003**, *100*, 3641-3646. DOI: 10.1073/pnas.0737142100

(20) Motomura, T.; Zuccarello, L.; Setif, P.; Boussac, A.; Umena, Y.; Lemaire, D.; Tripathy, J. N.; Sugiura, M.; Hienerwadel, R.; Shen, J. R. et al. An Alternative Plant-Like Cyanobacterial Ferredoxin with Unprecedented Structural and Functional Properties. *Biochim. Biophys. Acta* **2019**, *1860*, 148084. DOI: 10.1016/j.bbabio.2019.148084

(21) Berthomieu, C.; Boussac, A.; Mantele, W.; Breton, J.; Nabedryk, E. Molecular-Changes Following Oxidoreduction of Cytochrome-b559 Characterized by Fourier-Transform Infrared Difference Spectroscopy and Electron-Paramagnetic Resonance: Photooxidation in Photosystem II and Electrochemistry of Isolated Cytochrome B559 and Iron Protoporphyrin IX-Bisimidazole Model Compounds. *Biochemistry* **1992**, *31*, 11460-11471. DOI: 10.1021/bi00161a026

(22) Marboutin, L.; Boussac, A.; Berthomieu, C. Redox Infrared Markers of the Heme and Axial Ligands in Microperoxidase: Bases for the Analysis of C-type Cytochromes. *J. Biol. Inorg. Chem.* **2006**, *11*, 811-823. DOI: 10.1007/s00775-006-0119-4

(23) Marboutin, L.; Desbois, A.; Berthomieu, C. Low-Frequency Heme, Iron-Ligand, and Ligand Modes of Imidazole and Imidazolate Complexes of Iron Protoporphyrin and

Microperoxidase in Aqueous Solution. An Analysis by Far-Infrared Difference Spectroscopy. *J. Phys. Chem. B* **2009**, *113*, 4492-4499. DOI: 10.1021/jp810774g

(24) Dupeyrat, F.; Vidaud, C.; Lorphelin, A.; Berthomieu, C. Long Distance Charge Redistribution upon Cu,Zn-Superoxide Dismutase Reduction - Significance for Dismutase Function. *J. Biol. Chem.* **2004**, *279*, 48091-48101. DOI: 10.1074/jbc.M402728200

(25) Hasegawa, K.; Ono, T.; Noguchi, T. Ab Initio Density Functional Theory Calculations and Vibrational Analysis of Zinc-bound 4-methylimidazole as a Model of a Histidine Ligand in Metalloenzymes. *J. Phys. Chem. A* **2002**, *106*, 3377-3390. DOI: 10.1021/jp012251f

(26) Hienerwadel, R.; Berthomieu, C. Bicarbonate Binding to the Non-heme Iron of Photosystem II Investigated by Fourier Transform Infrared Difference Spectroscopy and 13C-Labeled Bicarbonate. *Biochemistry* **1995**, *34*, 16288-16297. DOI: 10.1021/bi00050a008

(27) Diaz-Moreno, I.; Hulsker, R.; Skubak, P.; Foerster, J. M.; Cavazzini, D.; Finiguerra, M. G.; Diaz-Quintana, A.; Moreno-Beltran, B.; Rossi, G. L.; Ullmann, G. M. et al. The Dynamic Complex of Cytochrome c(6) and Cytochrome f Studied with Paramagnetic NMR Spectroscopy. *Biochim. Biophys.Acta* **2014**, *1837*, 1305-1315. DOI: 10.1016/j.bbabio.2014.03.009

(28) Wallace, C. J. A.; Clarklewis, I. Functional Role of Heme Ligation in Cytochrome C. Effects of Replacement of Methionine-80 with Natural and Non-natural Residues by Semisynthesis. *J. Biol. Chem.* **1992**, *267*, 3852-3861.

(29) Mcknight, J.; Cheesman, M. R.; Thomson, A. J.; Miles, J. S.; Munro, A. W. Identification of Charge-Transfer Transitions in the Optical-Spectrum of Low-Spin Ferric Cytochrome-P-450 *Bacillus-Megaterium*. *Eur. J. Biochem.* **1993**, *213*, 683-687. DOI: 10.1111/j.1432-1033.1993.tb17808.x

(30) Nabedryk, E.; Berthomieu, C.; Vermeglio, A.; Breton, J. Photooxidation of High-Potential (C559, C556) and Low-Potential (C552) Hemes in the Cytochrome Subunit of Rhodopseudomonas-Viridis Reaction Center - Characterization by FTIR Spectroscopy. *FEBS Lett.* **1991**, *293*, 53-58. DOI: 10.1016/0014-5793(91)81151-W

(31) Schlereth, D. D.; Mantele, W. Redox-Induced Conformational-Changes in Myoglobin and Hemoglobin - Electrochemistry and Ultraviolet Visible and Fourier-Transform Infrared

Difference Spectroscopy at Surface-Modified Gold Electrodes in an Ultra-Thin-Layer Spectroelectrochemical Cell. *Biochemistry* **1992**, *31*, 7494-7502. DOI: 10.1021/bi00148a009

(32) Dorr, S.; Schade, U.; Hellwig, P. Far Infrared Spectroscopy on Hemoproteins: A Model Compound Study from 1800-100 cm^{-1}. *Vib. Spectrosc.* **2008**, *47*, 59-65. DOI: 10.1016/j.vibspec.2008.02.003

(33) Kitagawa T.; Ozaki Y. Infrared and Raman Spectra of Metalloporphyrins. In Buchler J.W. (eds) Metal Complexes with Tetrapyrrole Ligands I. Structure and Bonding. **1987** vol 64. Springer, Berlin, Heidelberg. DOI: 10.1007/BFb0036790

(34) Desbois, A. Resonance Raman-Spectroscopy of C-type Cytochromes. *Biochimie* **1994**, *76*, 693-707. DOI: 10.1016/0300-9084(94)90145-7

(35) Spiro, T. G.; Strekas, T. C. Resonance Raman-Spectra of Heme Proteins - Effects of Oxidation and Spin State. *J. Am. Chem. Soc.* **1974**, *96*, 338-345. DOI: 10.1021/ja00809a004

(36) Mileni, M.; Haas, A. H.; Mantele, W.; Simon, J.; Lancaster, C. R. D. Probing Heme Propionate Involvement in Transmembrane Proton Transfer Coupled to Electron Transfer in Dihemic Quinol : Fumarate Reductase by C-13-labeling and FTIR Difference Spectroscopy. *Biochemistry* **2005**, *44*, 16718-16728. DOI: 10.1021/bi051034s

(37) Moore, G. R.; Pettigrew, G. W.; Pitt, R. C.; Williams, R. J. P. pH-Dependence of the Redox Potential of Pseudomonas-Aeruginosa Cytochrome-C-551. Biochim Biophys Acta 1980, 590, 261-271. DOI: 10.1016/0005-2728(80)90030-4

(38) Moh, P. P.; Fiamingo, F. G.; Alben, J. O. Conformational Sensitivity of Beta-93 Cysteine Sh to Ligation of Hemoglobin Observed by FTIR Spectroscopy. *Biochemistry* **1987**, *26*, 6243-6249. DOI: 10.1021/bi00393a044

(39) Susi, H.; Byler, D. M.; Gerasimowicz, W. V. Vibrational Analysis of Amino-Acids - Cysteine, Serine, Beta-Chloroalanine. *J. Mol. Struct.* **1983**, *102*, 63-79. DOI: 10.1016/0022-2860(83)80007-6

(40) Li, H. M.; Thomas, G. J. Cysteine Conformation and Sulfhydryl Interactions in Proteins and Viruses .1. Correlation of the Raman S-H Band with Hydrogen-Bonding and Intramolecular Geometry in Model Compounds. *J. Am. Chem. Soc.* **1991**, *113*, 456-462. DOI: 10.1021/ja00002a012

(41) Becker, B., Felcyn, E.W., Herman, A., Pikies, J., Wojnowski, W. Schwingungsspektroskopische Untersuchungen der Acidität von Silanthiolen; quantitative Zusammenhänge zwischen der Struktur und den Dv(SH)-, HNP- und pK-Werten. *Z. Anorg. Allg. Chem.* **1982**, *488*, 229-234. DOI: 10.1002/zaac.19824880127

(42) David, J. G.; Hallam, H. E. Infra-Red Solvent Shifts. Part 8.-Acidity of Thiophenols. *Trans. Faraday. Soc.* **1964**, *60*, 2013-2016.

(43) Mielcarek, A.; Dolega, A. Weak Hydrogen Bonding Interaction S-H ··· O=C Studied by FT-IR Spectroscopy and DFT Calculations. *J. Mol. Struct.* **2016**, *1103*, 217-223. DOI: 10.1016/j.molstruc.2015.09.032

(44) Boucher, L. J.; Katz, J. J. Infared Spectra of Metalloporphyrins (4000-160 cm^{-1}). *J. Am. Chem. Soc.* **1967**, *89*, 1340-1345. DOI: 10.1021/ja00982a011

(45) Cornilsen, B. C.; Nakamoto, K. Metal Isotope-Effect on Metal-Ligand Vibrations .12. Imidazole Complexes with Co(Ii), Ni(Ii), Cu(Ii) and Zn(Ii). *J. Inorg. Nucl. Chem.* **1974**, *36*, 2467-2471.

(46) Hu, S. Z.; Mukherjee, A.; Piffat, C.; Mak, R. S. W.; Li, X. Y.; Spiro, T. G. Modeling the Heme Vibrational Spectrum: Normal-mode Analysis of Nickel(II) Etioporphyrin-I from Resonance Raman, FT-Raman, and Infrared Spectra of Multiple Isotopomers. *Biospectroscopy* **199**5, *1*, 395-412. DOI: 10.1002/bspy.350010605

(47) Kozlowski, P. M.; Rush, T. S.; Jarzecki, A. A.; Zgierski, M. Z.; Chase, B.; Piffat, C.; Ye, B. H.; Li, X. Y.; Pulay, P.; Spiro, T. G. DFT-SQM Force Field for Nickel Porphyrin: Intrinsic Ruffling. *J. Phys. Chem. A* **1999**, *103*, 1357-1366. DOI: 10.1021/jp9819700

(48) Oshio, H.; Ama, T.; Watanabe, T.; Kincaid, J.; Nakamoto, K. Structure Sensitive Bands in the Vibrational-Spectra of Metal-Complexes of Tetraphenylporphine. *Spectrochim. Acta A* **1984**, *40*, 863-870. DOI: 10.1016/0584-8539(84)80176-2

(49) Berthomieu, C.; Marboutin, L.; Dupeyrat, F.; Bouyer, P. Electrochemically Induced FTIR Difference Spectroscopy in the Mid- to Far Infrared (200 μm) Domain: A New Setup for the Analysis of Metal-Ligand Interactions in Redox Proteins. *Biopolymers* **2006**, *82*, 363-367. DOI: 10.1002/bip.20469

(50) Green, E. L.; Taoka, S.; Banerjee, R.; Loehr, T. M. Resonance Raman Characterization of the Heme Cofactor in Cystathionine beta-synthase. Identification of the Fe-S(Cys) Vibration in the Six-coordinate Low-spin Heme. *Biochemistry* **2001**, *40*, 459-463. DOI: 10.1021/bi0010874

(51) Argade, P. V.; Sassaroli, M.; Rousseau, D. L.; Inubushi, T.; Ikedasaito, M.; Lapidot, A. Confirmation of the Assignment of the Iron Histidine Stretching Mode in Myoglobin. *J. Am. Chem. Soc.* **1984**, *106*, 6593-6596. DOI: 10.1021/ja00334a024

(52) Kitagawa, T.; Nagai, K.; Tsubaki, M. Assignment of the Fe-Nepsilon (His F8) Stretching Band in the Resonance Raman-Spectra of Deoxy Myoglobin. *FEBS Lett.* **1979**, *104*, 376-378. DOI: 10.1016/0014-5793(79)80856-X

(53) Wells, A. V.; Sage, J. T.; Morikis, D.; Champion, P. M.; Chiu, M. L.; Sligar, S. G. The Iron Histidine Mode of Myoglobin Revisited - Resonance Raman Studies of Isotopically Labeled Escherichia-Coli Expressed Myoglobin. *J. Am. Chem. Soc.* **1991**, *113*, 9655-9660. DOI: 10.1021/ja00025a034

(54) Parker, S. F. Assignment of the Vibrational Spectrum of L-cysteine. *Chem. Phys.* **2013**, *424*, 75-79. DOI: 10.1016/j.chemphys.2013.04.020

(55) Matei, A.; Drichko, N.; Gompf, B.; Dressel, M. Far-infrared Spectra of Amino Acids. *Chem. Phys.* **2005**, *316*, 61-71. DOI: 10.1016/j.chemphys.2005.04.033

(56) Umemura, J. Vibrational-Spectra, Normal Coordinate Analyses, and Molecular Configurations of Crystalline Propionic-Acid. *J. Mol. Struct.* **1977**, *36*, 35-54. DOI: 10.1016/0022-2860(77)85004-7

(57) Bernardina, S. D.; Alabarse, F.; Kalinko, A.; Roy, P.; Chapuis, M.; Vita, N.; Hienerwadel, R.; Berthomieu, C.; Judeinstein, P.; Zanotti, J. M. et al. New Experimental Set-ups for Studying Nanoconfined Water on the AILES Beamline at SOLEIL. *Vib. Spectrosc.* **2014**, *75*, 154-161. DOI: 10.1016/j.vibspec.2014.07.016